Triangular pulse generation using a dual-parallel Mach–Zehnder modulator driven by a single-frequency radio frequency signal

Fangzheng Zhang, Xiaozhong Ge, and Shilong Pan*

Key Laboratory of Radar Imaging and Microwave Photonics, Ministry of Education, Nanjing University of Aeronautics and Astronautics, Nanjing 210016, China

**Corresponding author: pans@ieee.org*

Received August 19, 2013; revised September 27, 2013; accepted September 29, 2013; posted October 2, 2013 (Doc. ID 195995); published October 31, 2013

A simple scheme for the generation of full-duty-cycle triangular pulses is proposed and experimentally demonstrated using a dual-parallel Mach–Zehnder modulator driven by a single-frequency RF signal. By properly setting the bias voltages and the RF power, even-order harmonics in the optical intensity are suppressed, and the amplitude of the first-order harmonic is 9 times of that of the third-order harmonic. A periodical triangular pulse train is obtained in the time domain. 2.5, 5, and 10 GHz triangular pulse trains are experimentally generated, which verifies the feasibility of the proposed scheme.

OCIS codes: (060.4080) Modulation; (060.5625) Radio frequency photonics; (350.4010) Microwaves.
http://dx.doi.org/10.1364/OL.38.004491

Photonic generation of optical or radio frequency (RF) triangular pulses has attracted much attention because of its applications in all-optical signal processing and microwave photonic systems [1–3]. Many approaches have been proposed for generating a triangular shaped pulse in the optical domain [4–8]. A method based on spectrum shaping of ultrashort pulses followed by frequency-to-time mapping using a dispersive element is reported by several groups. The spectrum shaping can be done by either a spatial light modulator [4] or an optical spectrum shaper based on polarization devices [5]. The drawback of such schemes is that the use of ultrashort pulses leads to a high cost and the generated triangular pulse usually has a small duty cycle (<1). For many applications, triangular pulse trains with a full duty cycle (= 1) are preferable, e.g., a full-duty-cycle triangular pulse train can be used for doubling the pulses in both the frequency and time domains based on cross phase modulation and fiber dispersion [2]. Another category of photonic triangular pulse generation schemes is based on external modulation of a continuous wave (CW) light using electro-optical modulators [6–8]. The basic principle of this method is to manipulate the modulated optical sidebands such that the harmonics in the optical intensity approximately equal the Fourier components of a triangular pulse train. Full-duty-cycle triangular pulses can be generated using this method. In [6], a dual-electrode Mach–Zehnder modulator (DE-MZM) and a length of dispersion fiber are used to generate the triangular pulses, where the fiber is incorporated to suppress the unwanted fourth-order harmonic. By properly setting the bias voltage, the modulation depth of the DE-MZM and the fiber length, full-duty-cycle triangular pulses can be obtained. In [7], a single-drive MZM is used for optical suppressed-carrier modulation, and optical filtering as well as polarization manipulations follow to further adjust the amplitudes of the required harmonics. In addition to the modulator, other optical devices are needed in [6] and [7], which evidently increases the system complexity. In [8], only one dual-parallel MZM (DPMZM) is utilized for the triangular pulse generation, but two RF signals with different frequencies (f and $3f$) are required to drive the DPMZM. In addition, the methods proposed in [6–8] are only theoretically analyzed and verified through simulations. For better performance evaluation, it is highly desirable to perform experimental demonstrations of these schemes.

In this Letter, we propose and experimentally demonstrate a novel approach to generating triangular pulses using a DPMZM driven by a single-frequency RF signal. By properly setting the bias voltages, even-order harmonics of the optical intensity are suppressed, and by choosing appropriate powers of the RF signals to the DPMZM, the first- and third-order harmonics in the optical intensity compose a spectrum of a periodical triangular pulse train. The proposed scheme needs no other optical devices after the modulator. Compared with another reported method also utilizing a DPMZM [8], only a single-frequency RF signal is used, which apparently leads to significant system simplification. The principle of the scheme is theoretically analyzed, and its feasibility is verified by an experiment. Triangular pulse trains with repetition rates of 2.5, 5, and 10 GHz are successfully generated.

Figure 1 shows the configuration of the proposed scheme. The key device in the scheme is a DPMZM consisting of two child MZMs (MZM1 and MZM2), and a third parent MZM that is composed of MZM1 and MZM2. There are two RF inputs and three independent DC bias voltages. Let V_{rf1} and V_{rf2} represent the RF signals applied to MZM1 and MZM2, and V_{bias1}, V_{bias2}, and V_{bias3} denote the three bias voltages applied to MZM1, MZM2, and the parent MZM, respectively. When MZM1 and MZM2 operate at the chirp-free configuration, the output optical fields of MZM1 and MZM2 are [9]

$$E_1 = \frac{E_{\text{in}}}{\sqrt{2}} \cos\left[\frac{\pi}{2V_\pi}(V_{rf1}(t) + V_{\text{bias1}})\right] e^{j\frac{V_{\text{bias1}}}{2V_\pi}\pi}, \quad (1)$$

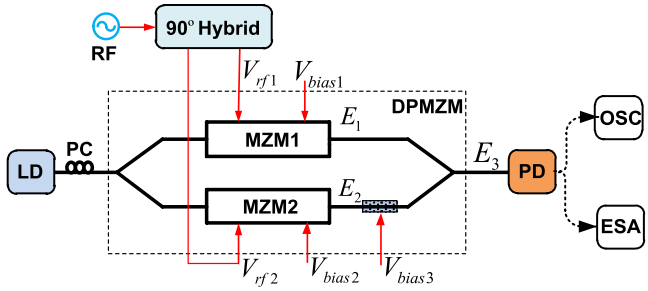

Fig. 1. Experimental setup of the proposed triangular pulse generator. LD, laser diode; PC, polarization controller; PD, photodetector; OSC, oscilloscope; ESA, electrical spectrum analyzer.

$$E_2 = \frac{E_{\text{in}}}{\sqrt{2}} \cos\left[\frac{\pi}{2V_\pi}(V_{rf2}(t) + V_{\text{bias2}})\right] e^{j\frac{V_{\text{bias2}}}{2V_\pi}\pi}, \quad (2)$$

where E_{in} is the optical field of the input CW light and V_π is the half-wave voltage of the MZMs. The optical field at the output of the DPMZM is written as

$$E_3 = E_1 + e^{j\frac{V_{\text{bias3}}}{V_\pi}\pi} E_2. \quad (3)$$

When this optical signal is sent to a photodetector (PD) for intensity detection, the output current of the PD is given by

$$\begin{aligned} I(t) = \Re E_3 E_3^* = \frac{\Re|E_{\text{in}}|^2}{2}\Bigg\{ & \cos^2\left[\frac{\pi}{2V_\pi}(V_{rf1}(t) + V_{bias1})\right] \\ & + \cos^2\left[\frac{\pi}{2V_\pi}(V_{rf2}(t) + V_{\text{bias2}})\right] \\ & + 2\cos\left[\frac{\pi}{2V_\pi}(V_{rf1}(t) + V_{\text{bias1}})\right] \\ & \times \cos\left[\frac{\pi}{2V_\pi}(V_{rf2}(t) + V_{\text{bias2}})\right] \\ & \times \cos\left(\frac{V_{\text{bias2}} - V_{\text{bias1}} + 2V_{\text{bias3}}}{2V_\pi}\pi\right)\Bigg\}. \end{aligned} \quad (4)$$

where $\Re$ is the responsivity of the PD. When V_{bias1}, V_{bias2}, and V_{bias3} are set to be $(2k + 1/2)V_\pi$, $(2m + 3/2)V_\pi$, and 0, respectively, where k and m are two integers, the third term in Eq. (4) equals zero. If the two RF signals have a phase difference of 90°, i.e., $V_{rf1}(t) = A\sin(2\pi ft)$ and $V_{rf2}(t) = A\cos(2\pi ft)$, where f is the frequency of the RF signal and A is the amplitude, Eq. (4) can be simplified and further expanded based on the Jacobi–Anger expansions,

$$\begin{aligned} I(t) &= \frac{\Re|E_{\text{in}}|^2}{4}\left\{2 - \sin\left[\frac{A\pi}{V_\pi}\sin(2\pi ft)\right] + \sin\left[\frac{A\pi}{V_\pi}\cos(2\pi ft)\right]\right\} \\ &= \frac{\Re|E_{\text{in}}|^2}{2}\left\{1 - \sum_{n=1}^{\infty} J_{2n-1}\left(\frac{A\pi}{V_\pi}\right)\sin[2\pi(2n-1)ft]\right. \\ &\quad \left. - \sum_{n=1}^{\infty}(-1)^n J_{2n-1}\left(\frac{A\pi}{V_\pi}\right)\cos[2\pi(2n-1)ft]\right\}, \end{aligned} \quad (5)$$

where J_n denotes the nth order of the first kind of Bessel function. It is known from Eq. (5) that even-order harmonics are removed and only the odd-order harmonics are present. For a small modulation depth, harmonics higher than the third order can be neglected, so Eq. (5) is simplified to

$$\begin{aligned} I(t) &\approx \frac{\Re|E_{\text{in}}|^2}{2}\left\{1 + J_1\left(\frac{A\pi}{V_\pi}\right)\cos(2\pi ft) - J_1\left(\frac{A\pi}{V_\pi}\right)\sin(2\pi f)\right. \\ &\quad \left. - J_3\left(\frac{A\pi}{V_\pi}\right)\cos(6\pi ft) - J_3\left(\frac{A\pi}{V_\pi}\right)\sin(6\pi ft)\right\} \\ &= \frac{\sqrt{2}\Re|E_{\text{in}}|^2}{2}\left\{\frac{\sqrt{2}}{2} + J_1\left(\frac{A\pi}{V_\pi}\right)\cos\left(2\pi ft + \frac{\pi}{4}\right)\right. \\ &\quad \left. + J_3\left(\frac{A\pi}{V_\pi}\right)\cos\left[3\left(2\pi ft + \frac{\pi}{4}\right)\right]\right\}. \end{aligned} \quad (6)$$

By tuning the RF power, the amplitudes of the first-and third-order harmonics in Eq. (6) can be changed. When $A\pi/V_\pi = 1.51$, or $A = 0.48\ V_\pi$, we get $J_1(A\pi/V_\pi) = 9J_3(A\pi/V_\pi)$ and

$$I(t) \propto \text{DC} + \cos\left(2\pi ft + \frac{\pi}{4}\right) + \frac{1}{9}\cos\left[3\left(2\pi ft + \frac{\pi}{4}\right)\right]. \quad (7)$$

Equation (7) is the Fourier expansion of a periodical triangular pulse train when harmonics higher than the third order are neglected [7]. Since the DC component and the first- and third-order harmonics contribute most to the spectral power of a triangular pulse train, triangular pulses can be thus generated in the time domain.

Figure 2 shows the simulation results for the generation of a 5 GHz triangular pulse train. The amplitude and phase properties of the optical fields E_1 and E_2 are shown in Figs. 2(a) and 2(b), respectively, and the waveform of the generated 5 GHz triangular pulse train is given in Fig. 2(c). Figure 2(d) shows the electrical power spectrum of the obtained 5 GHz triangular pulse train, where the even-order harmonics are suppressed and the power ratio between the 5 and 15 GHz components is 19.08 dB, indicating that the amplitude of the first-order harmonic is 9 times of that of the third-order harmonic.

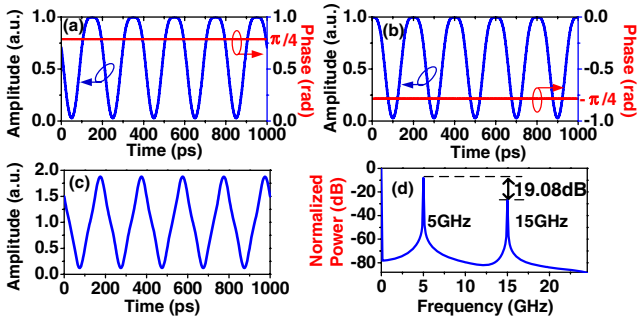

Fig. 2. Simulation results. The amplitude and phase of (a) E_1 and (b) E_2, (c) the generated 5 GHz triangular pulse train, and (d) the electrical power spectrum.

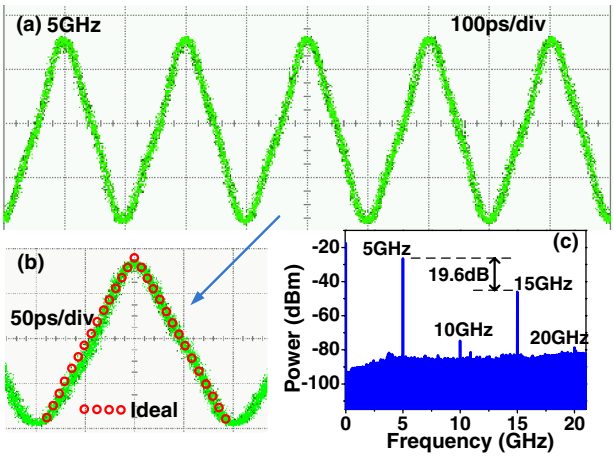

Fig. 3. (a) Waveform of the generated 5 GHz triangular pulse train, (b) the zoom-in view of the pulse, and (c) the electrical power spectrum of the triangular pulse train.

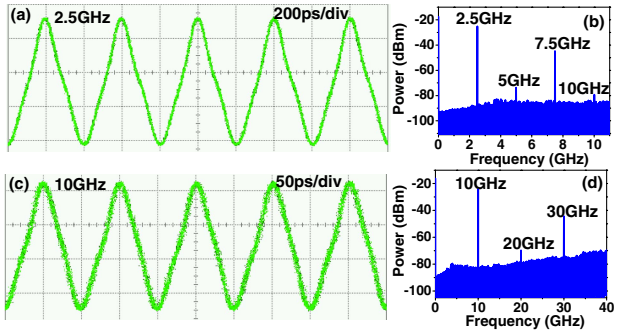

Fig. 4. Waveforms and electrical power spectra of the generated triangular pulse trains with repetition rates of (a), (b) 2.5 GHz and (c), (d) 10 GHz.

To further investigate the performance of the proposed scheme, an experiment is carried out based on the setup shown in Fig. 1. A CW light at 1550 nm from a laser diode is sent to a chirp-free DPMZM (Fujitsu FTM7962EP). The DPMZM has a half-wave voltage of 3.5 V at 22 GHz. An RF signal from a vector signal generator (Agilent E8267D) is divided by a broadband electrical 90° hybrid into two parts, then introduced to the two RF input ports of the DPMZM. After the DPMZM, a 50 GHz PD is utilized to perform optical-to-electrical conversion. The temporal waveform of the generated triangular pulse train is observed through an oscilloscope (Agilent 86100A) working with the average operation enabled, and the number of averages is 2. The spectral properties of the obtained pulse train are measured by an electrical spectral analyzer (Agilent E4447AU). In our scheme, feedback circuits are not used to solve the bias-drift problem with the DPMZM. However, no significant bias drift is observed during the experimental measurements.

Figure 3(a) shows the measured waveform of the generated 5 GHz triangular pulse train. To obtain Fig. 3(a), MZM1 and MZM2 are biased at $V_\pi/2$ and $-V_\pi/2$, respectively, and the vector signal generator is set to let the RF power at the output of the 90° hybrid be 15.8 dBm. The zoom-in view of the triangular pulse shape is shown in Fig. 3(b). It is found to be very close to an ideal triangular pulse shape. Figure 3(c) shows the electrical power spectrum of the 5 GHz triangular pulse train, where the powers of the 5, 10, 15, and 20 GHz components, i.e., the first-, second-, third-, and fourth-order harmonics, are −26.4 −74.6, −46, and −78.8 dBm, respectively. The power of the third-order harmonic is 19.6 dB lower than that of the first-order harmonic, which is very close to the theoretical result in Fig. 2(d). Furthermore, the powers of the second- and fourth-order harmonics are more than 25 dB lower than that of the third-harmonic, which indicates that the even-order harmonics are well suppressed.

The repetition rate of the obtained triangular pulse train can be changed by tuning the RF frequency. Considering that V_π of the DPMZM is slightly dependent on the frequency of the RF signal, the bias voltages and the RF power need to be slightly adjusted. When the RF frequency is tuned to 2.5 and 10 GHz, triangular pulse trains with repetition rates of 2.5 and 10 GHz are successfully generated, as shown in Figs. 4(a) and 4(c), respectively. The corresponding electrical power spectra are shown in Figs. 4(b) and 4(d), respectively. The powers of the first-order harmonics are 19.4 and 19.8 dB higher than those of the third-order harmonics, and the even-order harmonics are suppressed by more than 25 dB compared with the third-order harmonics.

In conclusion, we have proposed and experimentally demonstrated a simple triangular pulse generation scheme using a DPMZM. The scheme needs no optical filtering or dispersive element, and only a single-frequency RF signal is used to drive the DPMZM. Triangular pulse trains with repetition rates of 2.5, 5, and 10 GHz were experimentally generated.

This work was supported in part by the National Basic Research Program of China (2012CB315705), the National Natural Science Foundation of China (61107063), the Natural Science Foundation of Jiangsu Province (BK2012031), the Fundamental Research Funds for the Central Universities (NE2012002, NP2013101), and a Project Funded by the Priority Academic Program Development of Jiangsu Higher Education Institutions.

References

1. A. J. Seeds and K. J. Williams, J. Lightwave Technol. **24**, 4628 (2006).
2. A. I. Latkin, S. Boscolo, R. S. Bhamber, and S. K. Turitsyn, J. Opt. Soc. Am. B **26**, 1492 (2009).
3. M. Khan, H. Shen, Y. Xuan, L. Zhao, S. Xiao, D. E. Leaird, A. M. Weiner, and M. Qi, Nat. Photonics **4**, 117 (2010).
4. J. Chou, Y. Han, and B. Jalali, IEEE Photon. Technol. Lett. **15**, 581 (2003).
5. J. Ye, L. Yan, W. Pan, B. Luo, X. Zou, A. Yi, and S. Yao, Opt. Lett. **36**, 1458 (2011).
6. J. Li, X. Zhang, B. Hraimel, T. Ning, L. Pei, and K. Wu, J. Lightwave Technol. **30**, 1617 (2012).
7. J. Li, T. Ning, L. Pei, W. Jian, H. You, H. Chen, and C. Zhang, IEEE Photon. Technol. Lett. **25**, 952 (2013).
8. J. Li, T. Ning, L. Pei, W. Peng, N. Jia, Q. Zhou, X. Wen, and J. Chou, Opt. Lett. **36**, 3828 (2011).
9. Y. Li, J. Wu, Y. Ji, D. Kong, W. Li, X. Hong, H. Guo, Y. Zuo, and J. Lin, Opt. Express **20**, 24754 (2012).